

EXPERIMENTAL INVESTIGATION OF THE LEADING-EDGE ROUGHNESS ON THE BOUNDARY LAYER OF A PLUNGING AIRFOIL

F. Rasi Marzabadi*, M.R. Soltani**, M. Masdari

*Sharif University of Technology, Aerospace Research Institute, Tehran, Iran **Sharif University of Technology, Tehran, Iran

Keywords: *Plunging, roughness, wind turbine, transition, airfoil*

Abstract

Extensive experimental investigation was conducted to study the effect of leading-edge roughness on the state of the boundary layer of a wind turbine blade section. The application of surface grit roughness simulates surface irregularities that occur on the wind turbine blades. The measurements were done using multiple hot-film sensors and surface pressure transducers in both static and plunging oscillation of the airfoil. Frequency domain analysis was used to determine the state of the unsteady boundary layer.

1 Introduction

Dirt and contaminations accumulate on the wind turbine blade when it operates in the field. The main sources of contamination are insect compacts, ageing, sand impacts and the contaminations which come down with the rain. This contamination has a great role on the rotor performance. When insects, smog and dirt accumulate along the leading edge of the blade, power output can drop up to 40% of its clean value [1]. Surface roughness reduces the effectiveness of the airfoil. In this way the transition point moves toward the leading edge and causes early trailing edge turbulent separation [2]. The extent to which roughness affects airfoil performance is dependent on the nature of the roughness, its size relative to the boundary layer thickness, the Re number and the airfoil type. Roughness destabilizes the laminar boundary layer and weakens the turbulent boundary layer in regard to adverse pressure gradients. The corresponding effects on

airfoil lift and drag depend on the particular type of pressure distributions developed by the airfoil. The so-called laminar airfoils are particularly sensitive to roughness because the improved airfoil performance is obtained by tightly controlling the boundary layer behavior. Any deviations of the boundary layer from its intended behavior, such as that due to roughness, can result in significant deteriorations in performance.

Traditionally, there have been two avenues of roughness research: those researchers concerned with size and location of roughness and its effect upon airfoil transition location and performance, and those researchers concerned with the fluid dynamic mechanisms by which roughness affects the boundary-layer and surrounding flow-field [3]. For both types of research, the experiments have been conducted almost in static tests. However, wind turbines operate for most of their time in an unsteady flow environment. The forces on the blade element vary in time and space as a result of ambient turbulence, persistent shear in the ambient wind, blade flapping, structural response, control inputs, and skewed flow. Wind turbine airfoils operate frequently under fully separated flow when stall is used for power regulation at high wind speeds [4]. Most of the angle of attack changes that the rotor blades encounter are due to the variations in flapping and elastic bending of the blade, which can be closely modeled with a plunging type motion [5].

This study addresses some of the most important aspects of the leading edge roughness effect on the unsteady boundary layer of an

airfoil oscillating in plunge mode. The airfoil used in this study is a section of a 660 kW wind turbine blade under construction.

2 Experimental Apparatus

The experiments were conducted in the low speed wind tunnel in Iran. It is a closed circuit tunnel with rectangular test section of $80 \times 80 \times 200 \text{ cm}^3$. The test section speed varies continuously from 0 to 100 m/sec.

Two models with 25 cm chord and 80 cm span were used. They are the critical section of a 660 kW wind turbine blade under construction. Both models are exactly the same and were constructed of fiberglass with a measured accuracy of $\pm 0.1 \text{ mm}$. One of the airfoil models is equipped with 64 pressure orifices on the upper and lower surfaces. The pressure ports are located along the chord at an angle of 20 degrees with respect to the model span to minimize disturbances from the upstream taps, Fig. 1. Another model is equipped with eight hot-film sensors. The hot-films are special version of the flush-mounting DANTEC probe, Glue-on type. The sensor is deposited on a Kapton™ foil with thickness of about $50 \mu\text{m}$ which placed inside the fitted hole on the surface of the model in order to minimize the influence of probe thickness on transition. Its sensor is $0.9 \times 0.1 \text{ mm}$ and connected to a gold-plated lead area. The hot-films were located along the chord at an angle of 20 degrees with respect to the model span to minimize disturbances from the upstream one, Fig. 2. Hot-film data are obtained using constant temperature anemometer (CTA).

Data is transformed to the computer through a 64 simultaneous channel, 12-bit Analog-to-Digital (A/D) board capable of an acquisition rate of up to 1200 kHz.

To study the possible extent of performance loss due to the surface roughness, standard commercial grit (number 4 with thickness of 0.031 mm) was used to simulate surface contamination. Surface roughness was applied at $x/c=0.05$ using a 12mm double stick tape along the airfoil span, Fig. 3.

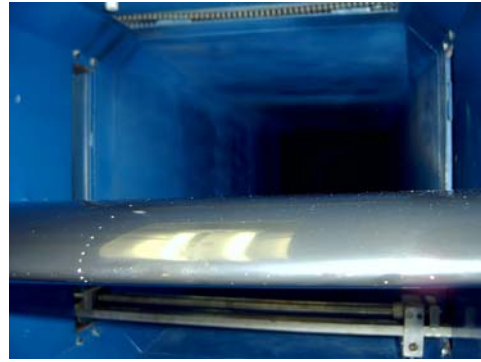


Fig. 1 Airfoil model along with the location of the pressure ports

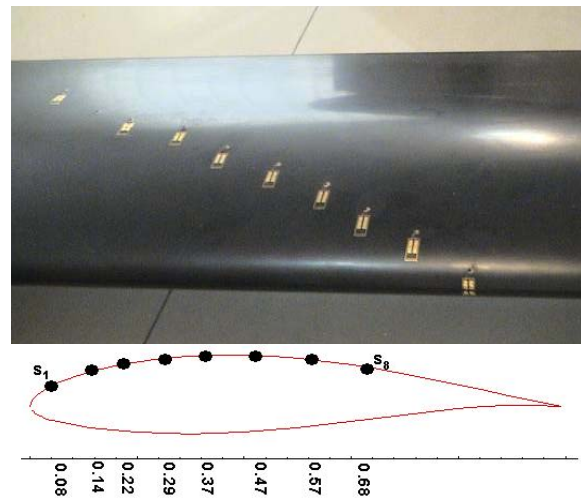


Fig. 2 Airfoil model along with the location of the hot-films



Fig. 3 Applied surface roughness

The plunging oscillation system oscillates the model at various amplitudes with frequencies ranging from 1 to 4 Hz. It incorporates a crankshaft to convert the circular motion of the motor to the reciprocal motion, which is transferred to the model by means of rods, Fig. 4. The pitch rotation point is fixed at about the wing quarter chord. The plunging displacement was varied sinusoidally as $h = \bar{h} \sin(\omega t)$.

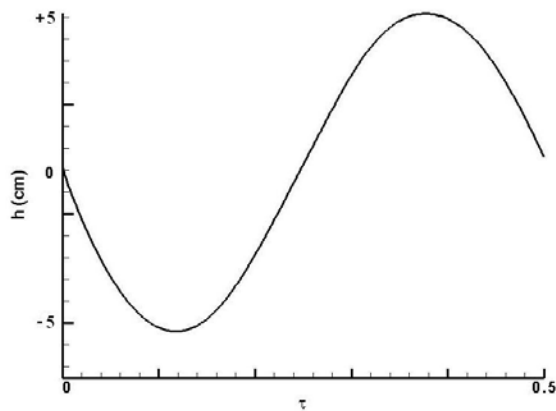
**EXPERIMENTAL INVESTIGATION OF THE LEADING-EDGE
ROUGHNESS ON THE BOUNDARY LAYER OF A PLUNGING AIRFOIL**

The plunging displacement was transformed into the equivalent angle of attack using the potential flow transformation formula, $\alpha_{eq} = k\bar{h} \cos(2\pi ft) + \alpha_0$. Figure 5 shows an example of the variation of the equivalent angle of attack for one oscillation cycle with respect to its corresponding time history of the plunging motion. It can be seen that α_{eq} is a maximum or a minimum whenever $h=0$ during down-stroke or upstroke portions of the motion, respectively.

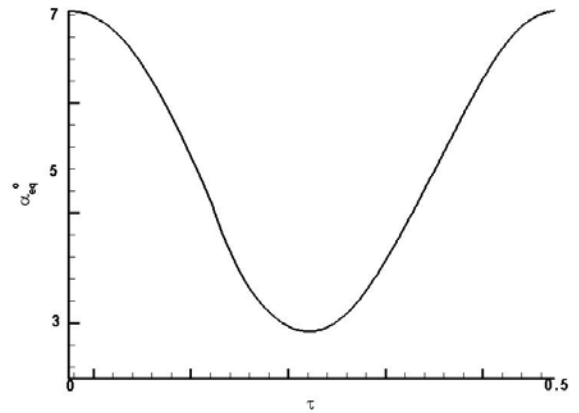
All experiments were conducted at Reynolds number of 0.42×10^6 , and a range of reduced frequencies, $k=0.03-0.1$ and at plunging amplitudes of ± 5 cm and ± 8 cm. In static tests the angles of attack were varied from -5 to 23 degrees.



Fig. 4 Oscillation device



a) Plunging displacement



b) Equivalent angle of attack

Fig. 5 Time history of the plunging motion and its corresponding equivalent angle of attack

3 Results and Discussion

The effect of leading edge roughness on pressure distribution around the airfoil is presented in Fig. 6. The results are shown for three static angles of attack of 5 , 10 , and 18 degrees which are below, within and beyond the static stall angle of attack of the model, respectively. Note that the static stall angle of attack for this particular model is about 11 degrees [6]. The transition location can almost be estimated from a sudden change in the slope of the pressure distribution which indicates the transition to turbulent through a separation bubble. The data clearly reveals that the flow transits as it passes over the roughness and becomes turbulent over the rest of the model. As indicated by arrows in Fig. 6a, at $\alpha=5^\circ$, the transition point moves from $x/c \approx 0.55$ to the roughness location at $x/c=0.05$, Fig. 6a. Note that the arrows are located at the beginning of the separation bubble, while in reality the flow becomes turbulent at a distance aft of the formation of the separation bubble. At higher angles of attack, it can be seen that the separated region over the model with roughness is more extensive than that of the clean one, Fig's 6b and 6c. Furthermore, the absolute value of C_p on the upper surface for the model with roughness is less than that of the clean one in all angles of attack which results in a sharp reduction in the lift data.

Figure 7 shows the composite dynamic plots of quasi-wall-shear stress, τ , calculated from un-calibrated hot-film signals in both clean and rough models. Variations of the equivalent angle of attack with time are shown on the top of the figures. The designated letters s_1 through s_8 shown on the right side of each trace are the hot-film responses in increasing order of chord wise positions, from about 8 to 68 percent of the chord. Based on the approach of Hodson [7] and Zhang [8], a quasi-wall-shear stress was defined

as: $\tau = \left(\frac{E^2 - E_0^2}{E_0^2} \right)^3$. Where E is the output

voltage of the hot-film sensor and E_0 is the offset voltage, zero-flow voltage at the air temperature encountered during the test. In this figure the model is set to mean angle of attack of 10 degrees and oscillates with reduced frequency of 0.08 and plunging amplitude of ± 8 cm. It is seen for the clean case that the signals of channels s_1 to s_4 , have smooth response with time which represents the laminar flow up to about 30% of the chord during the entire oscillation cycles, Fig. 7a. Thickening of the boundary layer causes reduction of the shear stress toward the trailing edge. The near-zero values of channel s_5 upholds the existence of laminar separation bubble at this location that causes transition of the boundary layer to occur further downstream toward the trailing edge. This is confirmed from the shear stress values of channel s_6 , which shows combinations of the laminar-turbulent flow. The values of shear stress vary from laminar to turbulent as the equivalent angle of attack increases during one oscillating cycle. As the equivalent angle of attack decreases, the flow again becomes laminar, Fig. 7a. The angles of attack in which the transition and relaminarization take place are not the same. The flow at the last two channels, s_7 and s_8 , is turbulent since the magnitude of the shear stress is increased and further the fluctuation amplitudes are relatively high, too. For the rough model, Fig. 7b, it can be seen that there is no sign of laminar flow in any channels. Because the flow transits to turbulent as it passes through the roughness, even the signal of channel s_1 show turbulent flow during entire one oscillating cycle. The quasi shear stress reduces

toward the trailing edge due to thickening of the turbulent boundary layer. The outputs of channels after s_6 toward the trailing edge show separated flow, Fig. 7b. Similar to the static result shown in Fig. 6, surface roughness causes early trailing edge turbulent separation in dynamic case.

Another approach for determining the boundary layer characteristics is through the frequency domain analysis. Figure 8 compares the Power Spectral Density (PSD) of the hot film signals in both rough and clean cases. For comparison the results are shown for the test conditions as previous figure. It can be seen that the first frequency of PSD's peak is about 2.3 Hz. Note that the oscillation frequency of this case is 3.1 Hz and it is expectable that the dominated frequency would be in the order of oscillation frequency. The other dominated frequencies are the sum of their previous frequency and the oscillation frequency. In the first two channels, Figs 8a and 8b, it is seen that the amplitudes of the spikes for the rough case are higher than that of the clean ones, especially at the higher frequency range of spectrum. It is confirmed that the flow is become turbulent on these channels in rough model but it is still laminar in clean one, as explained in Fig. 7. The plots of channels s_3 to s_6 , Figs 8c to 8f, reveal that for clean model, the amplitudes of the spikes are amplified with respect to the rough model and the spikes have their maximum amplitudes in channel s_5 for the clean case, Fig. 8e. The reason of this phenomenon is the growth of the boundary layer instability due to the boundary layer transition. In the last two channels, Figs 8g and 8h, it is seen that the amplitudes of the spikes for the rough model significantly grow which means the turbulent flow is separated widely from the trailing edge.

**EXPERIMENTAL INVESTIGATION OF THE LEADING-EDGE
ROUGHNESS ON THE BOUNDARY LAYER OF A PLUNGING AIRFOIL**

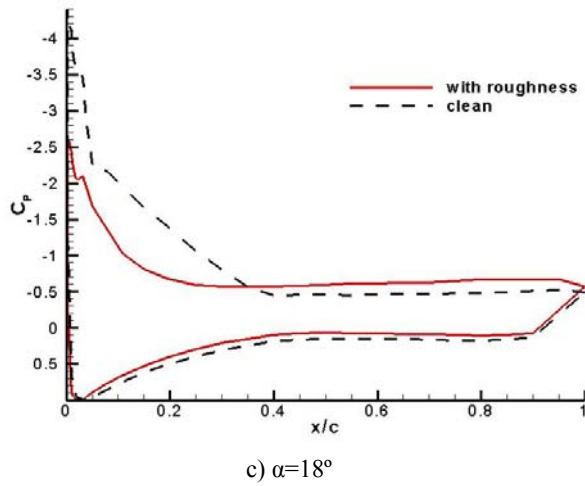
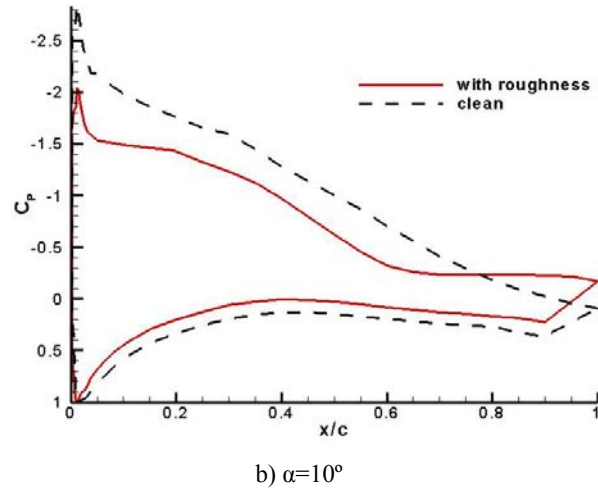
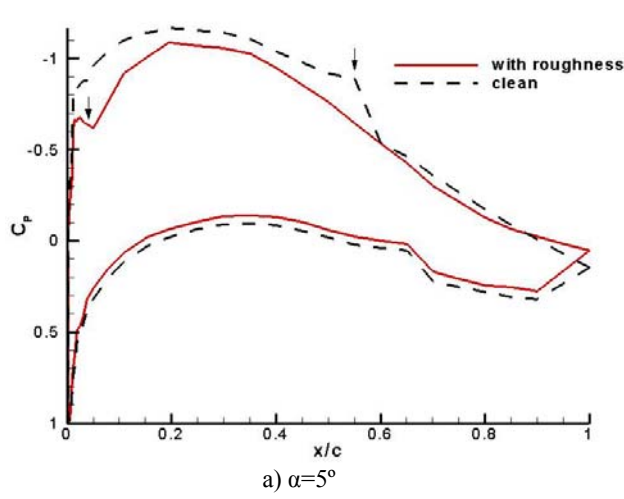


Fig. 6 The effect of leading edge roughness on the pressure distribution in static tests

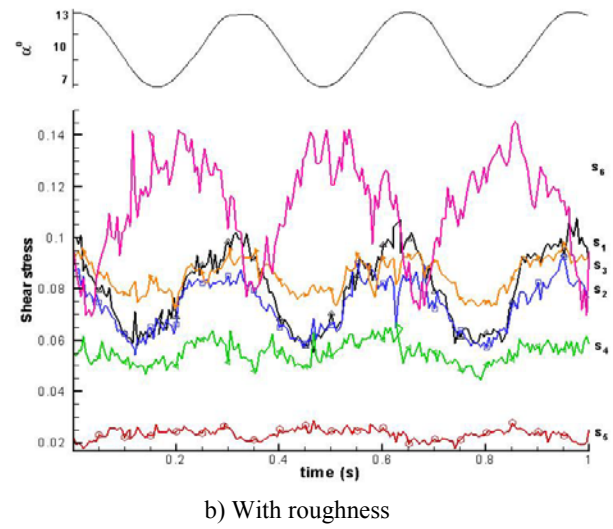
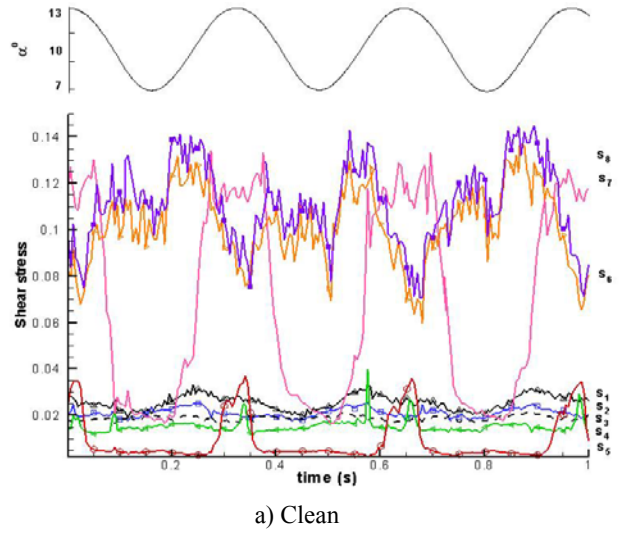
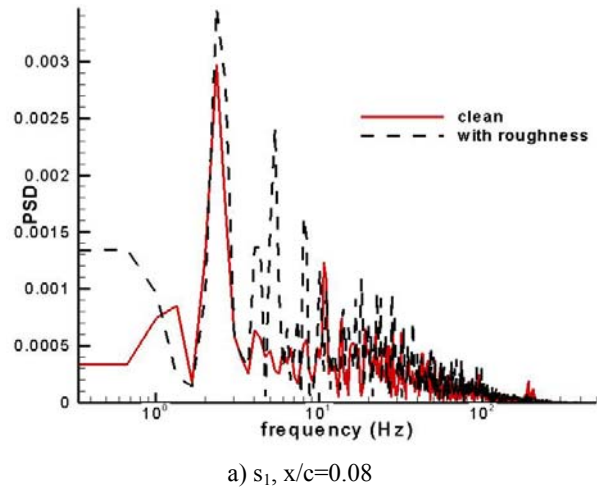
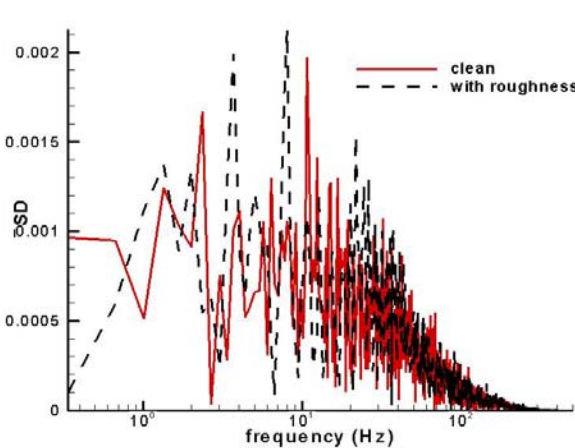
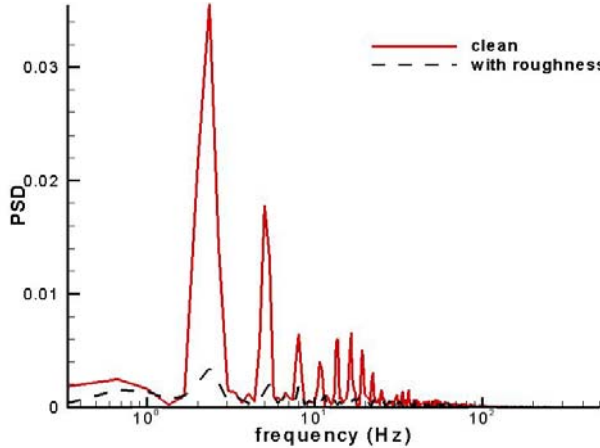


Fig. 7 Time history of quasi-wall-shear stress, $\alpha_0=10^\circ$, $k=0.08$

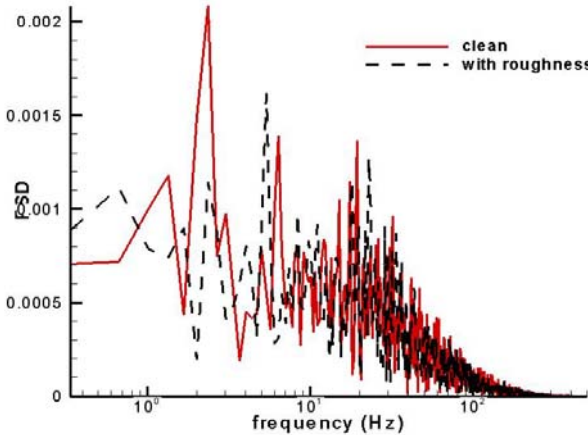




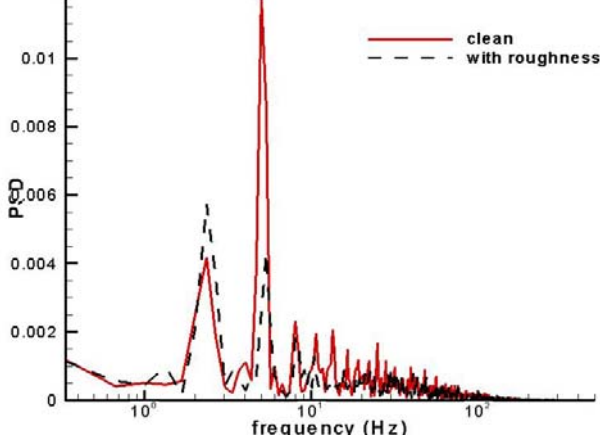
b) $s_2, x/c=0.14$



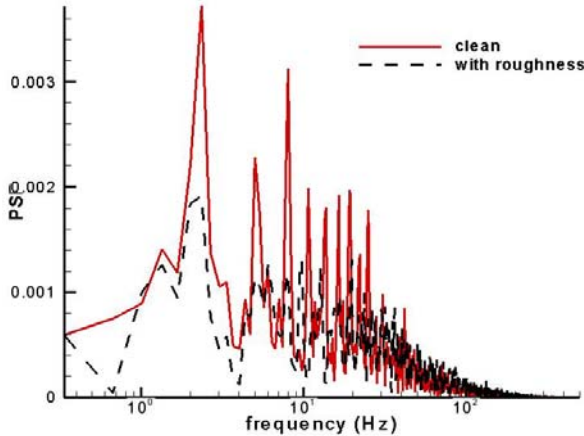
e) $s_5, x/c=0.37$



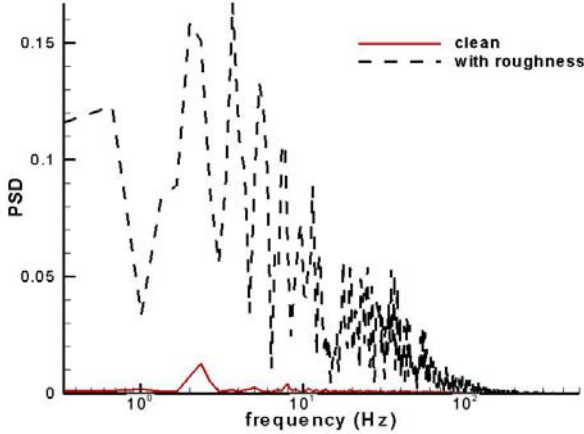
c) $s_3, x/c=0.22$



f) $s_6, x/c=0.47$



d) $s_4, x/c=0.29$



g) $s_7, x/c=0.57$

EXPERIMENTAL INVESTIGATION OF THE LEADING-EDGE ROUGHNESS ON THE BOUNDARY LAYER OF A PLUNGING AIRFOIL

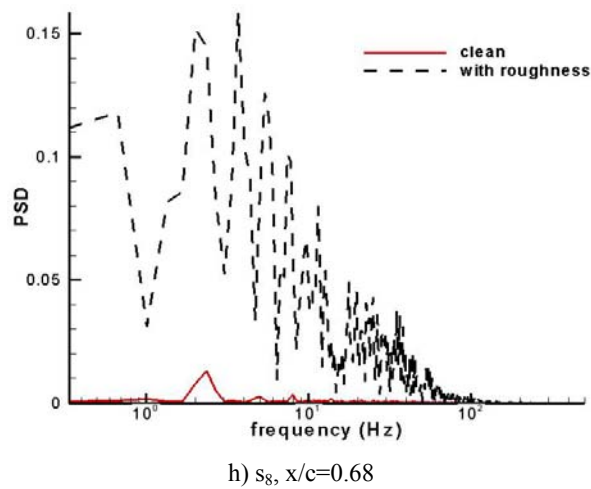


Fig. 8 Variations of the power spectral of hot film sensors, $\alpha_0=10^\circ$, $k=0.08$

4 Conclusions

To simulate surface contamination on the wind turbine blade, the effect of leading-edge roughness on the state of the boundary layer in both static and plunging oscillation was studied. Surface roughness moved the transition point toward the leading edge and caused early trailing edge turbulent separation which results in reducing the effectiveness of the airfoil. Frequency domain analysis showed that dominated frequencies of the boundary layer were a function of oscillation frequency and through transition, boundary layer instability frequencies were dominated with growth of the amplitudes of the spikes.

References

- [1] Hansen, AC, Butterfield, CP, Aerodynamics of Horizontal-Axis Wind Turbine. *Annual Review of Fluid Mechanics*, Vol. 25, pp.115-149, 1993.
- [2] Rooij, RPJOM, Timmer, WA, Roughness Sensitivity Considerations for Thick Rotor Blade Airfoils. *Journal of Solar Energy Engineering*, Vol. 125, 2003.
- [3] Kerho, MF, Effect of Large Distributed Roughness Near an Airfoil Leading-Edge on Boundary-Layer Development and Transition. *PhD Thesis*, University of Illinois at Urbana-Champaign, 1995.

- [4] Fuglsang, Peter, Antoniou, Ioannis, Sørensen, Niels N., and Madsen, Helge Aa., Validation of a Wind Tunnel Testing Facility for Blade Surface Pressure Measurements. *Risø-R-981(EN)*, 1998.
- [5] Tyler, C. Joseph, and Leishman, J. Gordon, Analysis of Pitch and Plunge Effects on Unsteady Airfoil Behavior. *Presented at the 47th annual forum of the American Helicopter Society*, 1991.
- [6] Soltani, MR and Rasi Marzabadi, F, Effect of Plunging Amplitude on the Performance of a Wind Turbine Blade Section. *The Aeronautical Journal*, Vol. 111, No. 1123, pp. 571-587, 2007.
- [7] Hodson, HP, and Howell, RJ, Unsteady Flow: Its role in the Low Pressure Turbine. *9th International Symposium Unsteady Aerodynamics, Aeroacoustics and Aeroelasticity of Turbomachines*, Lyon, 2000.
- [8] Zhang, XF, Mahallati, A, and Sjolander, SA, Hot-Film Measurements of Boundary Layer Transition, Separation and Reattachment on a Low Reynolds Numbers. *AIAA 2002-3643*, 38th AIAA/ASME/SAE/ASEE Joint Propulsion Conference & Exhibit, 2002.

Copyright Statement

The authors confirm that they, and/or their company or organization, hold copyright on all of the original material included in this paper. The authors also confirm that they have obtained permission, from the copyright holder of any third party material included in this paper, to publish it as part of their paper. The authors confirm that they give permission, or have obtained permission from the copyright holder of this paper, for the publication and distribution of this paper as part of the ICAS2010 proceedings or as individual off-prints from the proceedings.